


## Article

# On the Feasibility of Deep Geothermal Wells Using Numerical Reservoir Simulation

Ali Nassereddine and Luis E. Zerpa \* 

Petroleum Engineering Department, Colorado School of Mines, Golden, CO 80401, USA; nassereddine@mines.edu

\* Correspondence: lzerpa@mines.edu; Tel.: +1-303-384-2627

**Abstract:** This study examines the geothermal energy extraction potential from the basement rock within the Denver–Julesburg Basin, focusing on the flow performance and heat extraction efficiency of different geothermal well configurations. It specifically compares U-shaped, V-shaped, inclined V-shaped, and pipe-in-pipe configurations against enhanced geothermal system setups. Through numerical modeling, we evaluated the thermal behavior of these systems under various operational scenarios and fracture conditions. The results suggest that while closed-loop systems offer moderate temperature increases, Enhanced geothermal system configurations show substantial potential for high-temperature extraction. This underscores the importance of evaluating well configurations in complex geological settings. The insights from this study aid in strategic geothermal energy planning and development, marking significant advancements in geothermal technology and setting a foundation for future explorations and optimizations.

**Keywords:** geothermal; hot dry rock; reservoir modeling; numerical simulation; closed-loop geothermal; enhanced geothermal systems



**Citation:** Nassereddine, A.; Zerpa, L.E. On the Feasibility of Deep Geothermal Wells Using Numerical Reservoir Simulation. *Processes* **2024**, *12*, 1369. <https://doi.org/10.3390/pr12071369>

Academic Editor: Syed Muhammad Shakil Hussain

Received: 7 June 2024

Revised: 25 June 2024

Accepted: 27 June 2024

Published: 30 June 2024



**Copyright:** © 2024 by the authors. Licensee MDPI, Basel, Switzerland. This article is an open access article distributed under the terms and conditions of the Creative Commons Attribution (CC BY) license (<https://creativecommons.org/licenses/by/4.0/>).

## 1. Introduction

Geothermal energy, sourced from the Earth’s internal heat, offers a sustainable, low-carbon solution for continuous power generation, despite challenges in its extraction and utilization. As depicted in Figure 1, currently considered geothermal technologies vary with depth and temperature; shallow, hot areas might use conventional hydrothermal systems, while deeper, hotter regions may need enhanced geothermal systems (EGSs) that create permeable fracture networks for effective heat extraction. This highlights the necessity for innovative approaches in exploring and harnessing geothermal energy in challenging environments.

Maintaining optimal fluid flow rates is critical in geothermal energy extraction to prevent thermal breakthrough and sustain reservoir pressure, as highlighted in recent studies [1–3]. The strategic placement and configuration of production and injection wells are essential for managing these aspects without causing interference. Advanced reservoir engineering techniques, including simulation and monitoring, are increasingly vital for maximizing heat extraction and ensuring the longevity of the reservoir [4,5].

As the field of geothermal technology advances, ongoing research and innovative approaches, such as EGSs, are crucial. EGSs, recognized as a promising method for harnessing geothermal energy in low-permeability formations, involve creating permeability through hydraulic stimulation but must carefully consider potential issues like induced seismicity and environmental impacts [6].

The Denver–Julesburg (DJ) Basin, covering parts of Colorado, Wyoming, and Nebraska, presents untapped geothermal potential, especially in the Wattenberg field’s basement. This region, known for its high heat flow and thermal gradient, requires advanced drilling technologies due to its complex geology and deep reservoirs that can reach temperatures up to 572 °F (300 °C). Successful exploitation depends on a deep understanding

of subsurface geology, fluid dynamics, and reservoir characteristics such as porosity, permeability, and thermal properties, which are pivotal in determining the efficiency of heat extraction. In this work, we use the DJ Basin as a case study for the development of numerical reservoir simulation models to evaluate different geothermal well configurations to produce deep geothermal energy.

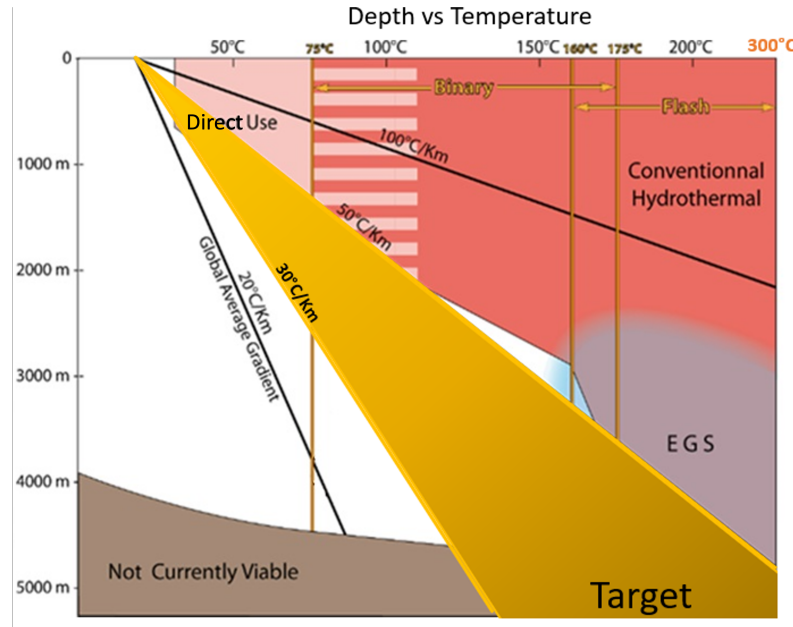


**Figure 1.** Temperature vs. depth plot illustrating possible geothermal gradients and their association with geothermal energy systems.

The DJ Basin, with its high geothermal gradients and complex geological features, offers significant potential for geothermal exploration [7,8]. The basin’s geothermal profile, as illustrated in Figure 2, shows a complex network of fault zones and cracked substrates favorable for Hot Dry Rock (HDR) systems. This cross-sectional view details the geological strata, fault zones, and potential HDR reservoirs, focusing on the Precambrian rocks in the Wattenberg field’s basement, which are key targets for geothermal exploitation.

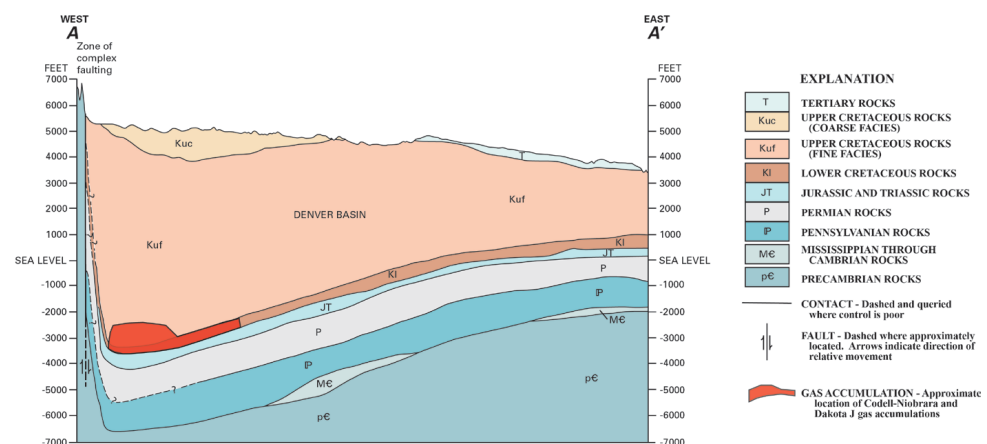


**Figure 2.** Map of the greater Wattenberg area, located within the Denver-Julesburg Basin of Colorado. West-east cross-section A-A’ showing the structural setting of the Denver Basin, Colorado, adapted from [9].

This work consists of a detailed reservoir simulation study to assess the geothermal energy extraction potential from deep wells in the Wattenberg field’s granitic basement of the DJ Basin. This study evaluates various well configurations and operational strategies,

specifically comparing closed-loop system designs, such as U-shaped, V-shaped, inclined V-shaped, and pipe-in-pipe (PIP) setups, against EGSs. Through numerical modeling, it explores the thermal dynamics under different operational conditions, focusing on the comparative efficacy of open-hole versus closed-hole systems and the potential of hybrid approaches combining closed-loop and EGS technologies. The findings aim to enhance the understanding of reservoir behavior, optimize energy output, and improve the longevity and performance of geothermal systems, thereby contributing to advanced geothermal resource development in complex geological settings like the DJ Basin, Colorado.

### *Geothermal Well Configurations*

The quest for efficient geothermal energy extraction continues to drive innovation, particularly in well configurations such as closed-loop systems (also known as advanced geothermal systems). Closed-loop (or conduction-based) geothermal systems (CLGSs) are artificial closed-loop circuits in which a working fluid is circulated and heated by the subsurface rock through conductive heat transfer [10]. The working fluid is contained within a metal pipe, preventing direct contact with the rock. This concept may be used for electricity generation or direct use near well locations. Innovations like heat transmission fluid recycling in horizontal wells offer high heat-mining rates in low-temperature geothermal reservoirs without complex hydro-fracturing, signaling a shift toward more sustainable solutions [11]. Multilateral well configurations in enhanced geothermal systems (EGSs) further exemplify significant progress, optimizing fluid-rock interactions for maximal heat extraction [12].

Additionally, advancements in horizontal wells, which generally yield better sweep efficiency than vertical wells, improve energy extraction by extending contact with the reservoir [13]. In EGSs, the integration of advanced drilling and fracturing techniques enhances heat output while managing thermal breakthrough risks, as shown in the Western Canada Sedimentary Basin [14]. The exploration of U-shaped and pipe-in-pipe closed-loop geothermal systems (CLGSs) by researchers such as Song et al. [15] and Bu et al. [16], alongside the coaxial closed-loop geothermal systems studied by Zhang et al. [17] and Wang et al. [18], introduced innovative approaches to address challenges like water loss and thermal short-circuiting, enhancing heat exchange efficiency.

This work expands on previous studies to explore the application of these innovative well configurations in deep HDR reservoirs, extending to depths up to 20,000 ft (6100 m), to model U-shaped, V-shaped, and pipe-in-pipe systems, as well as EGSs. This effort not only pushes the boundaries of geothermal research but also evaluates the feasibility, efficiency, and potential of these configurations in tapping into the Earth's deep thermal energy, making a substantial contribution to sustainable energy extraction.

## **2. Methodology**

This section presents the approach followed to build the numerical reservoir simulation models, including a review of the main rock and fluid properties, as well as descriptions of the different models used to evaluate the different geothermal well configurations.

### *2.1. Numerical Reservoir Simulation Approach*

Reservoir simulation is essential for understanding the behavior of geothermal reservoirs under various operational conditions, particularly in the granitic formations of the Wattenberg field, DJ Basin, Colorado. Utilizing numerical modeling, this research solves the conservation equations for mass, momentum, and energy across a discretized grid to analyze the interactions between the geothermal fluid, rock fractures, and rock matrix. The methodology aims to deepen our understanding of the physical and thermal characteristics of the reservoir. By simulating different operational scenarios, such as varying well layouts, fluid temperatures, and injection and production rates, we address key research questions to optimize geothermal energy extraction.

The simulation is grounded in a detailed understanding of the geological and geothermal properties of the Wattenberg field's granitic formations at a depth of 6100 m. Key parameters like permeability, porosity, thermal conductivity, specific heat, and the viscosity of high-temperature geothermal fluids (typically brine) are defined to model fluid movement and heat transfer in the reservoir. To focus on the deep formations, we insulate all production wells to minimize interference from shallower sedimentary layers, allowing a direct assessment of the deeper geothermal potential.

We test various operational scenarios, including adjustments to well layouts, fluid injection temperatures, and flow rates, to evaluate their impact on energy extraction. This detailed simulation process provides precise and meaningful insights, enhancing the prediction reliability and supporting the development of more efficient and sustainable geothermal systems in the DJ Basin.

Our simulation utilizes a Cartesian grid oriented along the I, J, and K axes, with dimensions of 141, 59, and 86 blocks, respectively. This setup ensures a detailed representation near critical wellbore locations to enhance thermal dynamics modeling (Figure 3). Each block, identified by a User Block Address (UBA), is key for achieving model convergence and accurately depicting temperature variations within the rock matrix. The reservoir simulator was built using the commercial software STARS version 2022 by Computer Modeling Group (CMG, Calgary, AB, Canada).

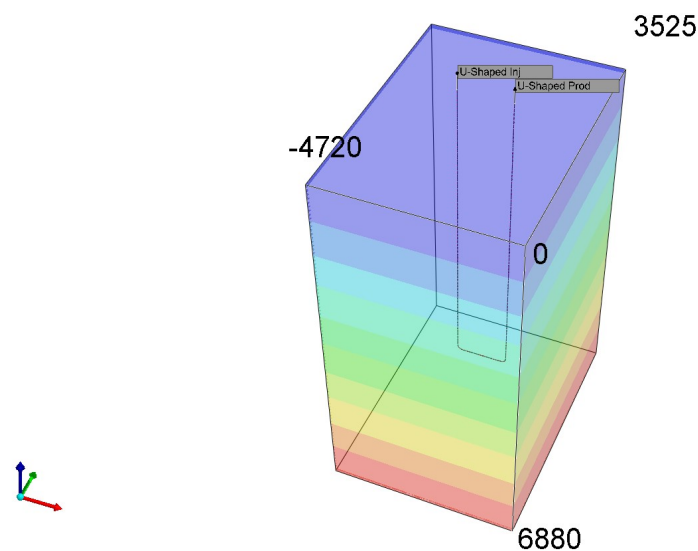


**Figure 3.** Geothermal reservoir 3-dimensional model, indicating global coordinates and injection and production wells location within the model.

For our geothermal reservoir simulations, we simplify the fluid-rock interaction, treating reservoir properties as constants. The porosity is set at 1% and permeability at  $1e-6$  millidarcies, with 100% water saturation assumed across the reservoir. The hydrostatic pressure gradient and rock compressibility are critical to the simulation's foundational parameters, established at  $10 \text{ kPa/m}$  and  $4.35 \times 10^7 \text{ kPa}^{-1}$ , respectively, which are crucial for accurate pressure distribution modeling within the reservoir (Table 1).

The thermal behavior of the reservoir is modeled using best-case scenario properties based on recent studies by Frash et al. [19], which recommend a formation volumetric heat capacity of  $2,667,500 \text{ J}/(\text{m}^3 \cdot ^\circ\text{C})$  and a thermal conductivity of  $252,720 \text{ J}/(\text{m} \cdot \text{day} \cdot ^\circ\text{C})$ .

These properties are integral to our understanding of the heat transfer dynamics within the reservoir, applied alongside a working fluid volumetric heat capacity of  $53,500 \text{ J}/(\text{m} \cdot \text{day} \cdot ^\circ\text{C})$ . The simulation uses freshwater as the working fluid, with the properties configured to the high-temperature conditions of the geothermal reservoir (Table 2).

**Table 1.** Input parameters for the reservoir and grid section.

Parameter	Value
Porosity	0.01
Permeability	$1 \times 10^{-6}$ md
Water saturation	100%
Hydrostatic gradient	10 kPa/m
Rock compressibility	$4.35 \times 10^{-7}$ kPa <sup>-1</sup>
Formation thermal conductivity	252,720 J/(m·day·°C)
Formation volume heat capacity	2,667,500 J/(m <sup>3</sup> ·°C)
Working fluid volume capacity	53,500 J/(m·day·°C)
Temperature gradient	50 °C/km

**Table 2.** Component properties for simulation.

Parameter	Value
AVISC	0.0047352 cp
BVISC	2760.26 °F
Reference pressure	8850 psi
Reference temperature	572 °F
Surface pressure	14.7 psi
Surface temperature	68 °F

The initial conditions reflect the geothermal and pressure environment of the deep subsurface targeted for exploration, establishing a consistent baseline for the simulation's phase equilibrium studies (Table 3).

**Table 3.** Parameters for initial conditions.

Parameter	Value
Reference pressure	8850 psi
Reference depth	20,000 ft

Geomechanical interactions were not explicitly modeled to focus on the thermal dynamics and fluid flow within the wells, consistent with the operational premise of closed-loop and EGS configurations. This comprehensive approach allows for detailed analysis and optimization of geothermal energy extraction strategies within the Wattenberg field's granitic formations, providing valuable insights into enhancing efficiency and sustainability.

The exclusion of geomechanical interactions simplifies the modeling process, allowing for a more focused analysis of the thermal dynamics and fluid flow within the reservoir. Geomechanical interactions would affect the results obtained for EGS models only, as the fracture conductivity may change due to temperature differences.

## 2.2. Well Configurations and Fluid Dynamics

This section explores the detailed configurations of the wells within each model, emphasizing the importance of distinct well types and their operational parameters for optimizing fluid dynamics in energy extraction processes.

### 2.2.1. U-Shaped Closed-Loop Geothermal System (CLGS) Model Description

The U-shaped CLGS represents an innovative approach designed for efficient geothermal energy extraction from HDR reservoirs. It employs an injection and production well pair, connected at the target depth by a lateral or horizontal well section. This system features a single continuous pipe for contained fluid flow, configured in a U-shape to promote continuous heat transfer by thermal conduction to the flowing fluid from the reservoir rock, thereby simplifying construction and reducing costs while preventing the fluid from being in direct contact with the rock formation (Figure 4).

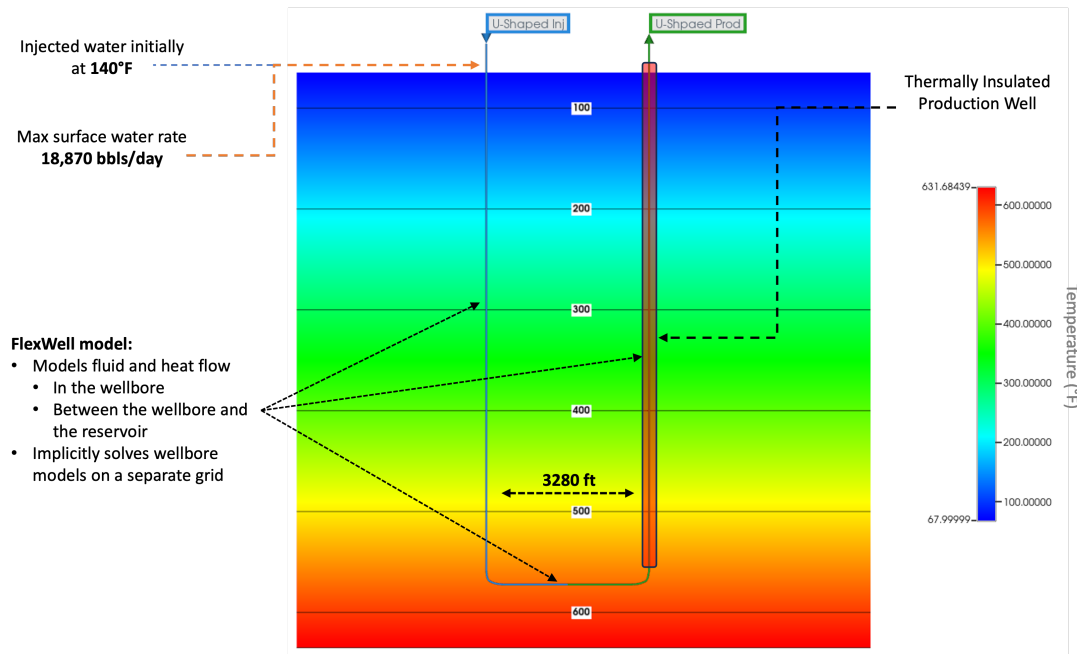


**Figure 4.** U-shaped closed-loop well model depiction.

The injection segment of the U-shaped model, termed the “injector”, initiates at the surface and extends deep into the geothermal system, aligned with the refined grid blocks to ensure accurate fluid dynamics modeling. This well starts from UBA (48, 17, 1) and extends horizontally after reaching UBA (48, 17, 77), continuing to UBA (67, 17, 77). Categorized as an injection well, it is designed to handle a maximum surface water rate of 3000 m<sup>3</sup>/day with a standardized well radius of 0.14 m for uniformity across the model.

Similarly, the “producer” well mirrors the “injector” in terms of trajectory and operational parameters but functions to extract the heated fluid. It stretches from UBA (87, 17, 1) to UBA (87, 17, 76) and connects horizontally to UBA (67, 17, 77), maintaining the system’s fluid balance with identical operational conditions to the injector. The production well is insulated to preserve the thermal energy extracted from deep within the reservoir. This insulation is crucial for minimizing heat losses across the extended horizontal reach, ensuring efficient heat exchange.

The injected fluid temperature is 140 °F, with a steam quality of 0, under a pressure of 1000 psi, optimized for the geothermal conditions of the model.

The FlexWell configuration is integral for accurately simulating the thermal and fluid mechanics of the U-shaped model. It involves specifying the casing properties and diameter for both the “injector” and “producer” wells to ensure consistent and accurate modeling within the FlexWell framework (Table 4).

**Table 4.** Diameter specifications for FlexWells.

Well	Wall Inner Diameter (ID)	Wall Outer Diameter (OD)
Injector	0.14 m	0.152 m
Producer	0.14 m	0.152 m

To simulate enhanced thermal conductivity, an alternative version of the U-shaped CLGS was developed by creating hydraulic fractures surrounding the lateral (horizontal) section of the U-shaped CLGS. Within the fractures of the U-shaped CLGS model, we introduced a highly thermally conductive material, increasing its thermal conductivity from a conventional value of 53,500 J/(m·day·°C) to 6.48 × 10<sup>6</sup> J/(m·day·°C). In the Results section, we present a comparison between the conventional U-shaped CLGS and the alternative version enhancing the thermal conductivity toward the lateral section of the CLGS.

### 2.2.2. Pipe-In-Pipe (PIP) Closed-Loop System Model Description

The PIP consists of a dual-pipe configuration within a single borehole. The system features two primary wells: the “casing” well as the outer section for injection and the inner “tubing” well as the producer. Both wells handle a maximum surface water rate of 3000 m<sup>3</sup>/day. The “casing” well has a radius of 0.14 m, while the “tubing” well has a narrower radius of 0.076 m, optimizing fluid dynamics. The injected fluid temperature is 140 °F, with a steam quality of 0 and an operating pressure of 1000 psi. The system includes the FlexWell model feature for dynamic simulation of the well interactions (Figure 5).

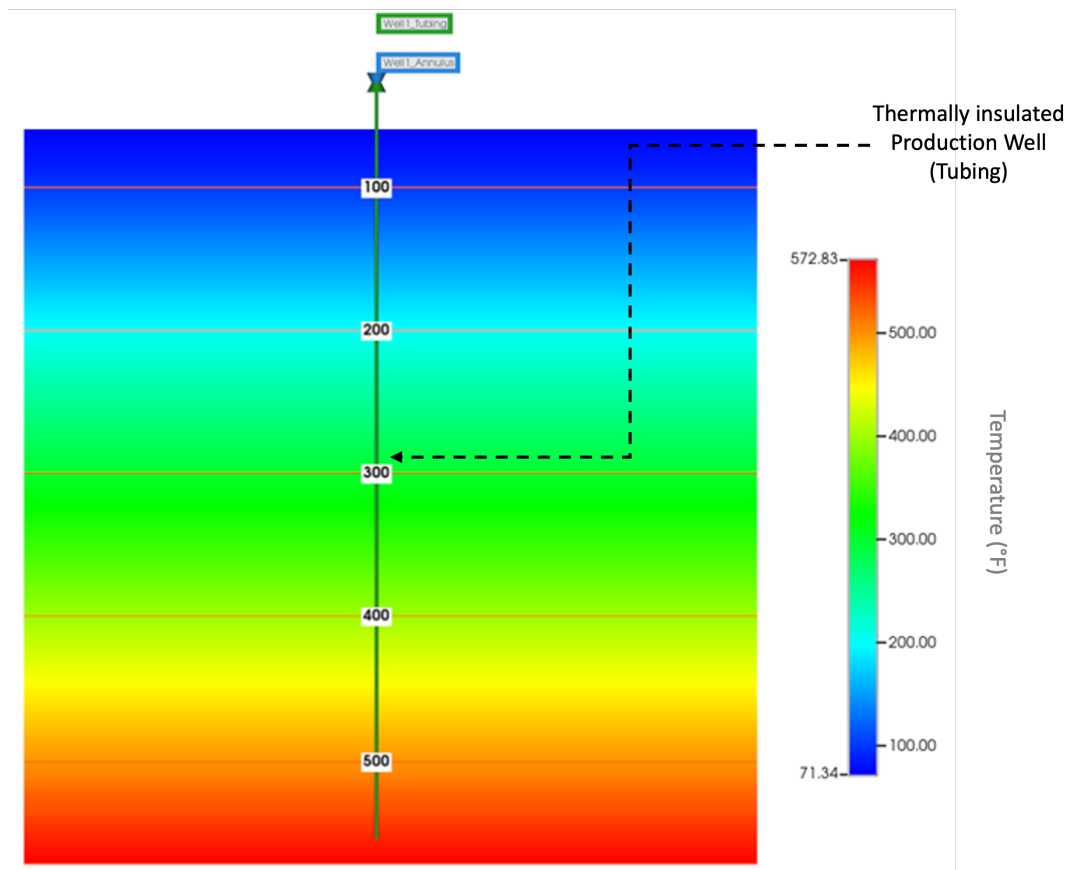


**Figure 5.** Pipe-in-pipe closed-loop well model description.

The inner “tubing” well is thermally insulated, with an inner diameter of 0.076 m and an insulated outer diameter of 0.102 m. This setup ensures an accurate representation of the operational dynamics and thermal behavior, maximizing the heat retention of the produced fluids while allowing heat transfer to the injected fluids flowing in the outer annular space.

### 2.2.3. V-Shaped Closed-Loop System Model Description

The V-shaped closed-loop system, also known as the U-shaped extended horizontally (USEH) model, marks a significant advancement in geothermal well design. This system is specifically engineered to maximize the extraction of geothermal energy from the high-temperature zones of HDR reservoirs by incorporating horizontal extensions at considerable depths (Figure 6).

In the V-shaped model, wells descend vertically to a depth of 20,000 ft, reaching high-temperature regions ideal for energy extraction. At this depth, each well extends 1968 ft horizontally, increasing the contact area between the heat transfer fluid and the geothermally heated rock, thereby enhancing heat absorption. This V-shaped configuration underscores the strategic placement and operational control of wells to maximize geother-

mal energy extraction efficiency, significantly improving the system’s heat absorption capacity and energy output.

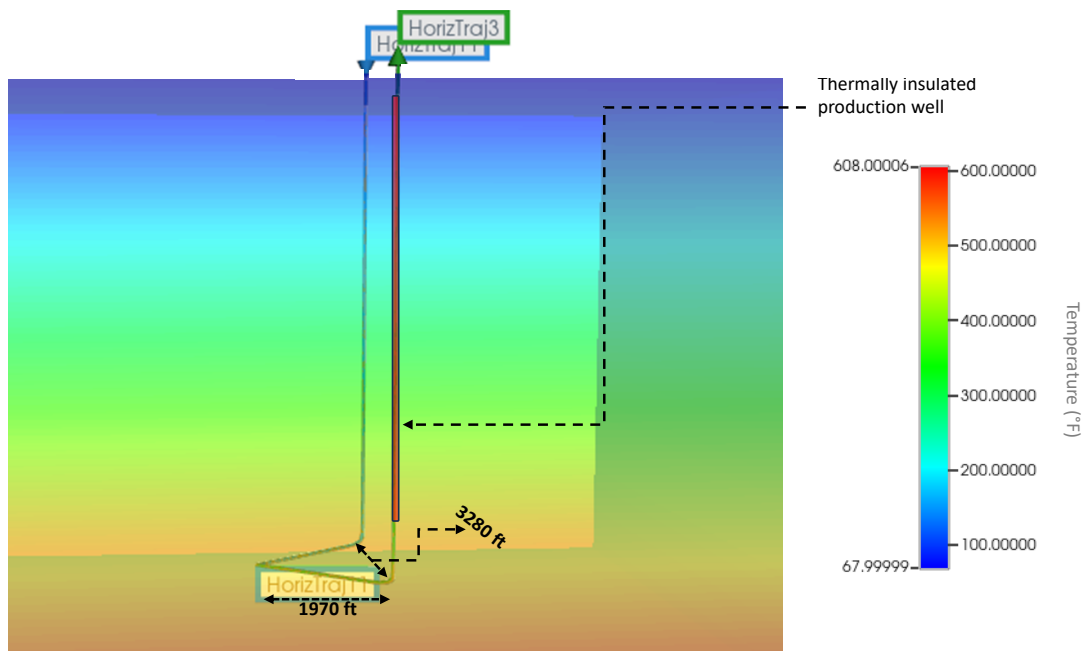


Figure 6. V-shaped closed-loop well model description.

#### 2.2.4. Inclined V-Shaped Closed-Loop System Model Description

The inclined V-shaped model is a refined geothermal well configuration designed to enhance heat extraction from HDR reservoirs. This model begins with two wells 3280 ft apart on the surface, descending vertically to a depth of 17,180 ft before diverging into an inclined lateral section of 3440 ft, reaching a total depth of 6100 m where reservoir temperatures are around 574 °F (Figure 7). This unique geometry increases the thermal contact surface area between the heat transfer fluid and the surrounding rock, boosting the system’s heat recovery capacity.

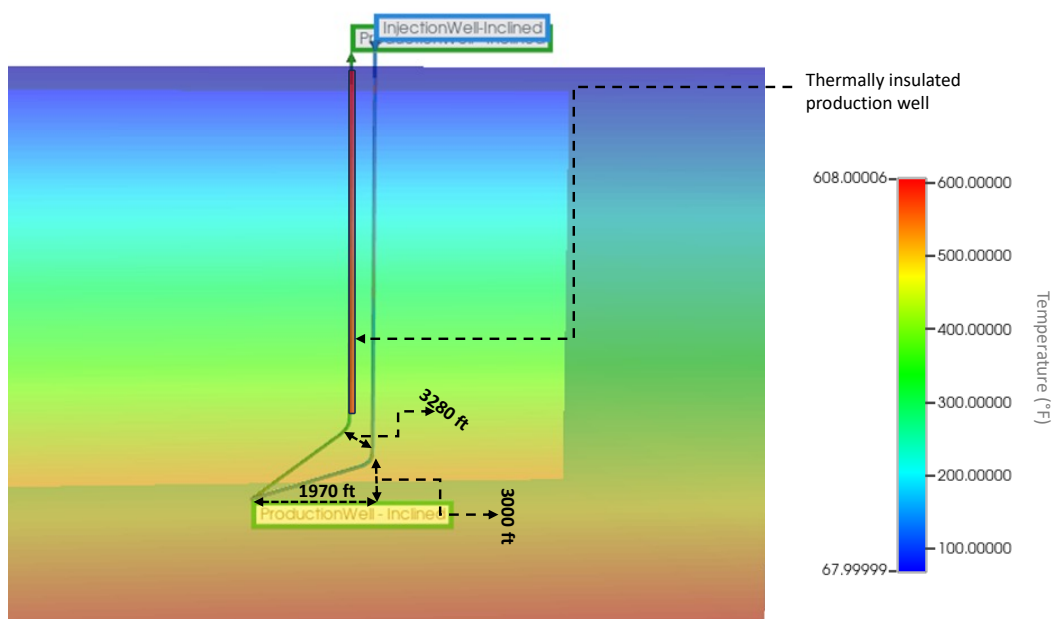


Figure 7. Inclined V-shaped closed-loop well model’s geometric configuration.



### 2.2.5. Enhanced Geothermal System (EGS) Model Description

The EGS model employs a progressive approach to maximize heat extraction in geothermal energy systems. This model uses engineered hydraulic fractures to increase reservoir permeability and establish extensive heat transfer pathways.

The injector well, the primary fluid entry point, is designed to inject water at a specific rate and temperature to maximize heat absorption. It starts from UBA (47, 12, 1) and extends horizontally to UBA (47, 36, 77), with a maximum surface water rate of 3000 m<sup>3</sup>/day and a well radius of 0.14 m. The producer well, extending from UBA (87, 12, 1) to UBA (87, 36, 77), parallels the injector to efficiently transport the heated fluid to the surface, following similar operational parameters (Figure 8).

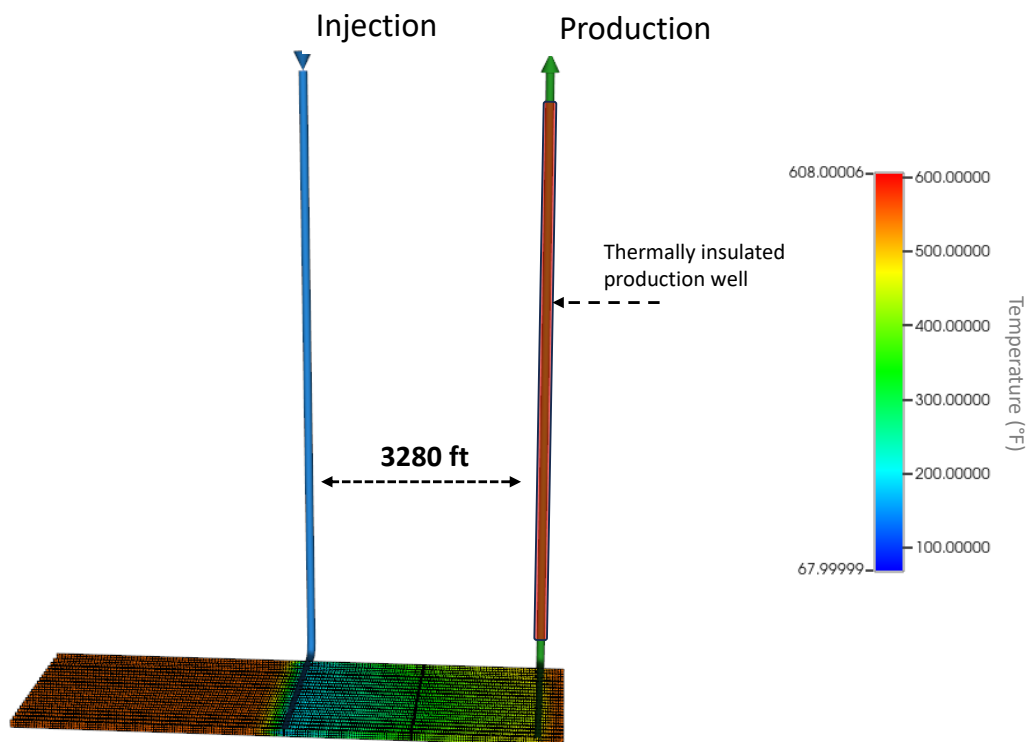


**Figure 8.** EGS well model depiction.

The initial setup includes defining the perforation intervals for both the injector and producer wells to optimize fluid flow and heat exchange, ensuring precise modeling and effective heat retrieval. This integration enhances simulation fidelity and highlights the EGS model's potential to significantly improve the efficiency and output of geothermal energy systems.

### 2.2.6. Inclined Enhanced Geothermal System (EGS) Model Description

The inclined EGS model offers a strategic adaptation within enhanced geothermal systems, employing an inclined configuration to address technical drilling challenges in deep-seated geothermal resource areas. This approach is particularly beneficial in regions where vertical drilling is impractical due to complex geological structures or obstructions.

In the inclined EGS model, wells reach a true vertical depth of 6100 m, accessing a high-temperature zone. Beyond this depth, the wells extend horizontally for 1000 m at the bottom of the geothermal gradient, traversing the hottest parts of the HDR formation to maximize thermal interaction and energy transfer (Figure 9).

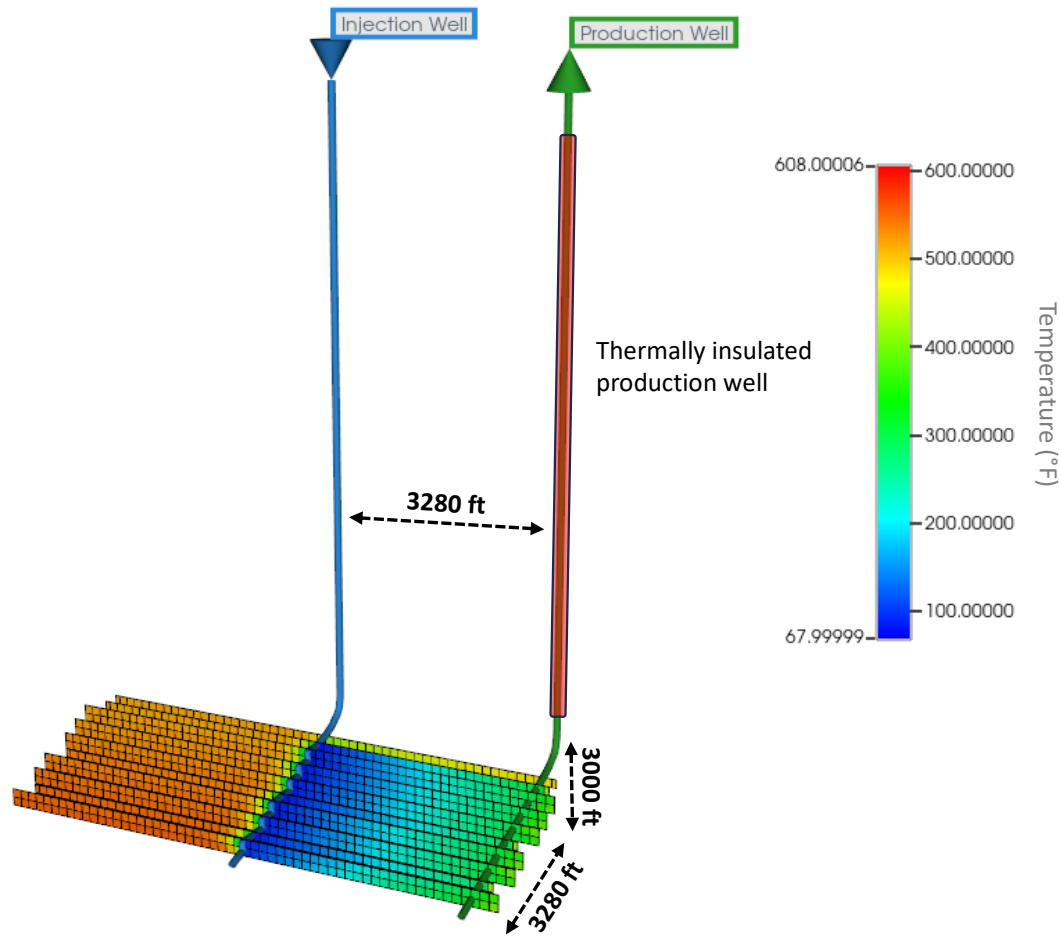


Figure 9. Inclined EGS well model depiction.

### 3. Results

Our simulation models are built on a robust foundation, integrating key parameters and insights from seminal research within the geothermal energy domain. We adopted critical thermal parameters, such as rock and cement thermal conductivities, and specific heat capacities from the work of Frash et al. [19], essential for modeling the thermal dynamics between geothermal fluids and reservoir formations. This integration aided in optimizing our models for advanced and enhanced geothermal systems.

Additional foundational data from Won et al. [20] on the thermal and mechanical properties of casing materials inform our simulations, enhancing the accuracy of our models in predicting the thermal and mechanical stability of geothermal wells.

Our models also draw from the work of Norbeck and Latimer [21], who provided a commercial-scale demonstration of enhanced geothermal systems (EGSs). Their real-case scenario serves as a benchmark for the verification of the reservoir simulation model built in this study. When comparing the field demonstration data with the simulation results, a 3% deviation in the production well temperature was compared, which is considered a good estimate (Figure 10).

This validation extended to temperature, pressure, and flow rate comparisons, confirming the calibration of the reservoir simulation model (Figure 11).

The following subsections present an analysis of the simulation results obtained from studying various geothermal well configurations over a period of 20 years.

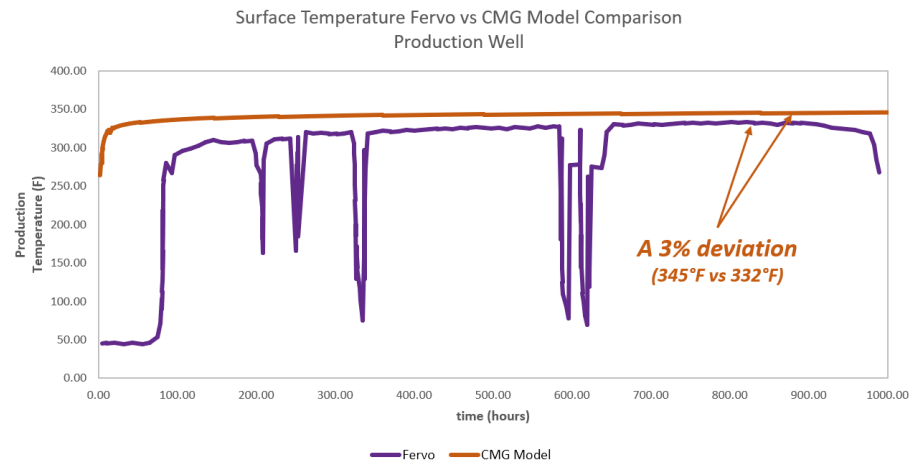


**Figure 10.** Fervo field demonstration data vs. reservoir simulation results in terms of produced surface temperature.

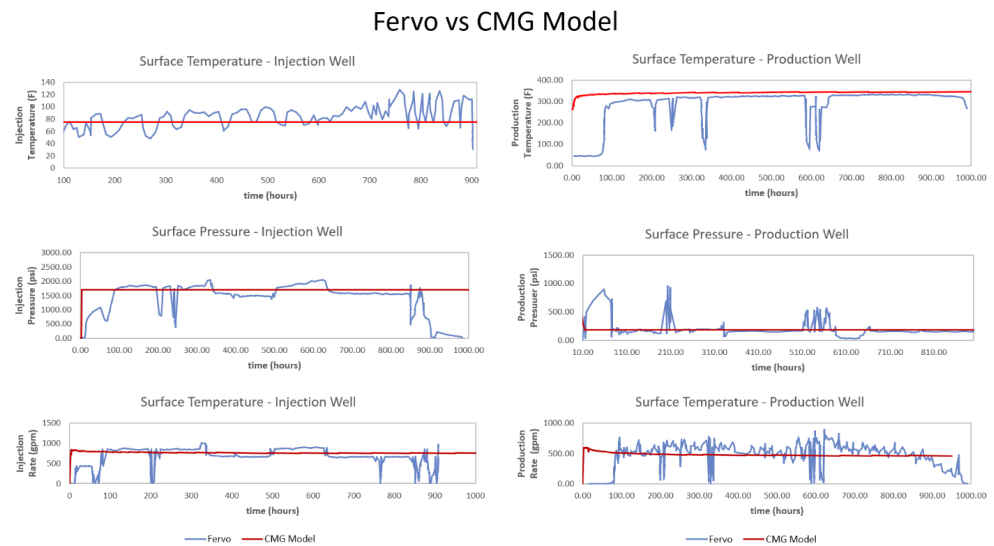


**Figure 11.** Fervo field demonstration data vs. reservoir simulation results in terms of surface temperature, pressure, and flow rate of injection and production wells.

### 3.1. Long-Term Performance Analysis of U-Shaped CLGS Well Model

Figure 12 shows the reservoir temperature distribution obtained by the U-shaped CLGS model after 20 years of injecting cold fluid and producing heated fluid. The horizontal lines represent the isotherms corresponding to the original geothermal gradient. The horizontal nature of the isotherms changes at the location of the well trajectory, indicating a change in the rock temperature surrounding the wells due to heat transfer from the rock to the flowing fluid. Over time, the change in the shallower isotherm indicates an increase in the rock temperature because the injected and produced fluid has a higher temperature than the rock at shallow depths. For the deeper isotherms, we can see a decrease in the rock temperature over time at the well locations. Heat is being transferred by conduction from the rock to the well, heating up the flowing fluid. We can also observe a decrease in temperature at the lateral portion of the well connecting the injection and production wells, indicated by a horizontal section with a lighter (yellow) color at 20,000 ft. The lateral well connecting the injection and production wells significantly enhances heat absorption by providing residence time to the flowing fluid at this deep and hot part of the formation.

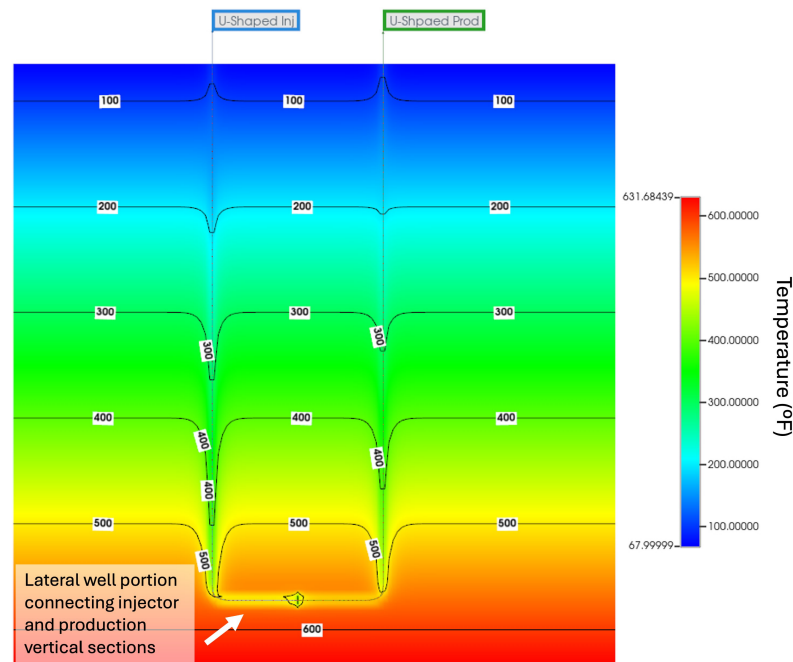


**Figure 12.** U-shaped closed-loop wells' reservoir temperature distribution after 20 years.

After 20 years, the model estimated a final production temperature of 183 °F compared to the injected fluid's temperature of 140 °F, illustrating a temperature gain. Figure 13 presents the temperature distribution for the injection and production wells, including the lateral well portion. Both the injection and production wells show an increase in fluid temperature along the direction of flow (the fluid in the injection well is flowing downward, while the fluid in the production well is flowing upward). The temperature profiles exhibit a curvature at shallow depths, where the injected fluid flowing downward cools down and then heats up with depth, while the produced fluid flowing upward cools down slightly, transferring heat to the rock at shallower depth. Notably, water, the sole working fluid in this model, remains in the liquid phase under operational conditions. Overall, the U-shaped model combines effective heat extraction with simplicity of design and operational feasibility, maintaining high temperatures over extended periods and ensuring stable temperature and pressure profiles. This reliability positions it as a promising option for sustained geothermal energy extraction and broader application in direct-use geothermal projects. Figure 14 presents the estimated pressure distribution for the injection and production wells, including the lateral well portion. The pressure increases with depth for both wells due to the hydrostatic fluid column within the wells, with the pressure in the production well being lower than that in the injection well due to friction losses.

### 3.2. Long-Term Performance Analysis of the Fractured U-Shaped CLGS Model

This section evaluates the impact of introducing a highly thermally conductive material into the hydraulic fractures surrounding the lateral (horizontal) section of the U-shaped CLGS to simulate enhanced thermal conductivity. By increasing the thermal conductivity of the fluid within the fractures from a conventional value of 53,500 J/(m·day·°C) to  $6.48 \times 10^6$  J/(m·day·°C), the fractured U-shaped CLGS model enhanced the thermal conductivity toward the lateral section of the CLGS.

First, the wells were hydraulically isolated from the reservoir rock by containing the fluid within the well tubulars, preventing any exchange between the injected fluid and the reservoir fluids. Over 20 years of operation, the model estimated a produced fluid temperature of 189 °F, slightly higher than the produced fluid temperature of 183 °F obtained with the base U-shaped CLGS model. A second version was evaluated by opening the well perforations, allowing direct interaction between the injected water and the fluids within the hydraulic fractures, significantly impacting the well's thermal profile due to the

higher conductivity inside the fractures. This configuration led to a temperature increase of approximately 23%, reaching 225 °F (Figure 15).

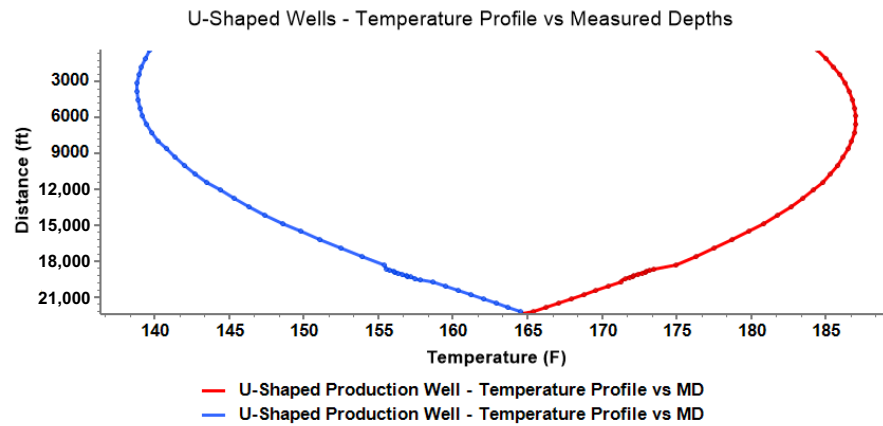


Figure 13. Estimated temperature profiles as a function of the measured depth for the injection and production wells, including the lateral well portion, in the U-shaped CLGS.

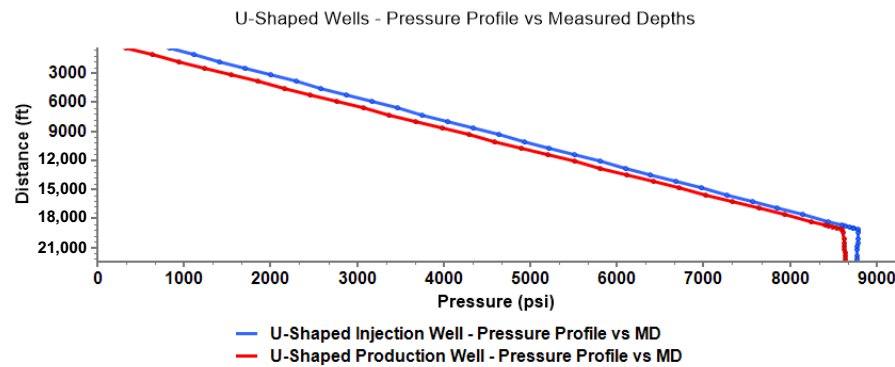


Figure 14. Estimated pressure profiles as a function of the measured depth for the injection and production wells, including the lateral well portion, in the U-shaped CLGS.

Comparing both configurations, the introduction of a highly conductive material had a minimal impact on the closed U-shaped well system, maintaining an average temperature of 189 °F over 20 years. However, the open fracture model exhibited a significant temperature increase to an average of 225 °F, underscoring that open fractures can considerably boost heat transfer. This indicates potential advantages for enhancing thermal recovery processes, emphasizing the critical role of fracture management in optimizing geothermal well performance.

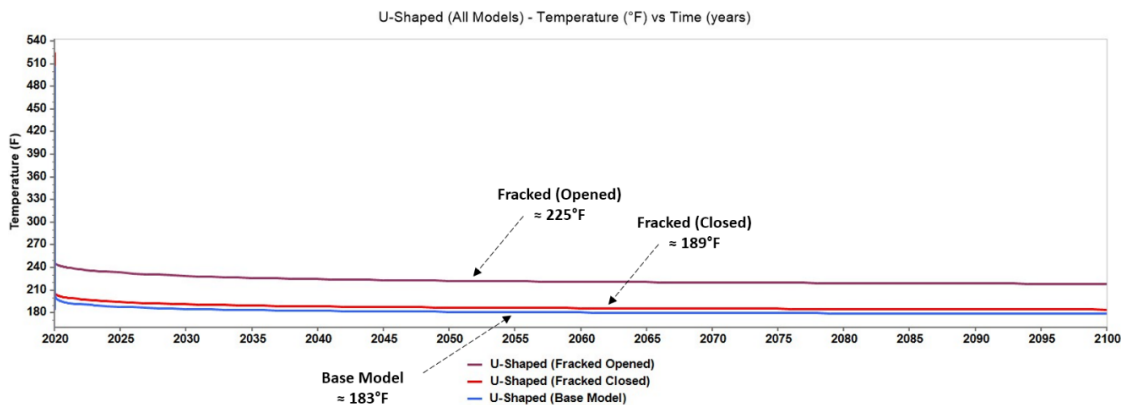
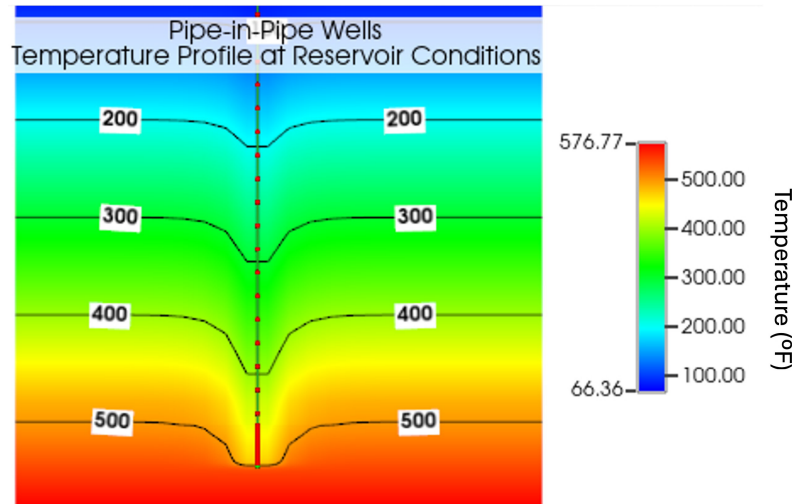


Figure 15. Produced surface temperature (°F) vs. time (years) for all U-shaped models.

### 3.3. Long-Term Performance Analysis of Pipe-In-Pipe (PIP) Geothermal Well Models

The PIP closed-loop well model, which consists of a dual-pipe configuration, demonstrates suboptimal performance in heat extraction from deep formations. The absence of a lateral section, which in models like the U-shaped CLGS extends the residence time of flowing fluids at the target depth, is a primary factor in its underperformance (Figure 16).



**Figure 16.** Reservoir temperature distribution after 20 years of operation for the PIP closed-loop well configuration.

In this case, the injected fluid does not effectively harvest the reservoir heat, leading to a low increase in the produced temperature to 146 °F after 20 years of operation from an injected fluid temperature of 140 °F. This minimal increase in temperature underscores the model’s inefficiencies, as the concentric design of the production well within the injection well reduces the contact area with the targeted formation, thus diminishing heat transfer by thermal conduction. The estimated temperature profiles for the injection and production wells with the measured depth are presented in Figure 17. The injected fluid initially loses heat at shallow depths, and then its temperature increases, reaching a maximum temperature of 161 °F at 20,000 ft. The temperature of the produced fluids (flowing upward) decreases along the direction of flow due to heat transfer to the surrounding annular space with the injected fluid, even with the thermally insulated tubing. The produced fluid temperature profile, influenced by the concentric tubing design, shows reduced heat extraction compared to the U-shaped model. The PIP model’s design limitations significantly impact its efficiency.

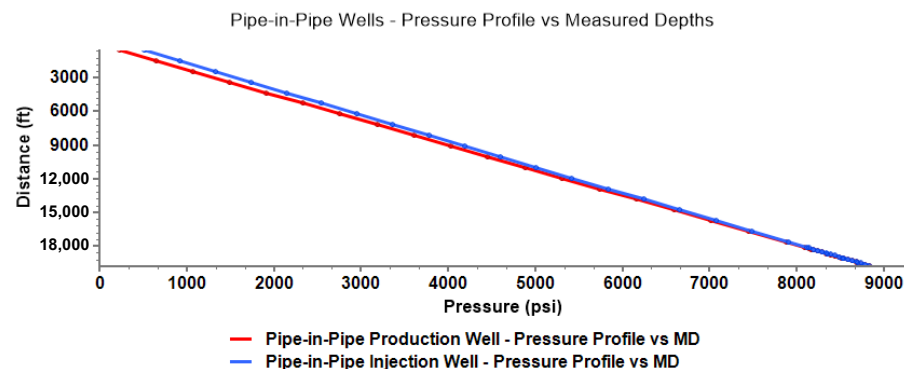


**Figure 17.** Estimated temperature profiles as a function of the measured depth for the PIP well configuration.

### 3.4. Long-Term Performance Analysis of V-Shaped Closed-Loop Model

The V-shaped closed-loop model extends the lateral section connecting the injection and production wells, effectively absorbing heat from the target formation at 20,000 ft, as represented by the reservoir temperature distribution map in Figure 18, where the lighter colors (yellow) indicate a lower temperature of the rock surrounding the V-shaped lateral section of the well. Its larger lateral section compared to the U-shaped base model significantly improves the contact between the wells and the formation, optimizing heat extraction for closed-loop systems.

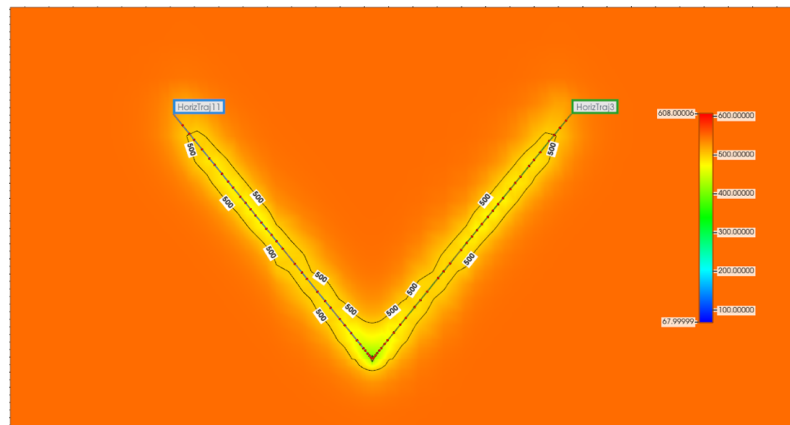


**Figure 18.** Reservoir temperature distribution after 20 years of operation for the V-shaped closed-loop well configuration.

After 20 years of simulation, the model estimated a produced fluid temperature of 185 °F, a notable increase from the injected fluid temperature of 140 °F. Figure 19 shows the temperature profiles for the injection and production wells of the V-shaped closed-loop configuration. For the injected fluid, there is a minor decrease in temperature near the surface at shallow depths, and then the temperature increases with depth. For the produced fluid, the temperature increases along the direction of flow (upward flow), with slight heat losses at shallow depths. The heat transfer primarily occurs through the casing walls, suggesting an indirect contact between the water and the reservoir rock. Like other models, the V-shaped system uses water as the working fluid, with its properties under various operational states confirming that water remains in the liquid phase throughout. The V-shaped model slightly outperforms the U-shaped model due to its extended contact area with the hot rock formation, leading to a higher produced temperature.

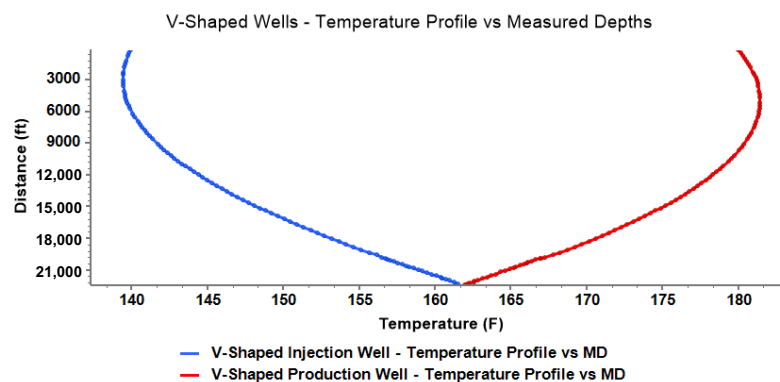


**Figure 19.** Estimated temperature profiles as a function of the measured depth for the injection and production wells, including the V-shaped lateral well portion).

### 3.5. Long-Term Performance Analysis of Inclined V-Shaped Geothermal Well Models

The inclined V-shaped closed loop leads to a lower produced temperature than the U-shaped and V-shaped models because the departure of the lateral V-shaped section starts at a shallower depth of 17,180 ft. The model effectively utilizes the heat around the injection and production wells (Figure 20), but the reduced contact of the lateral well section with the maximum depth of 6100 m at 572 °F makes the produced fluid temperature lower than the closed-loop systems where the lateral section is at the target depth (i.e., U-shaped and V-shaped cases).

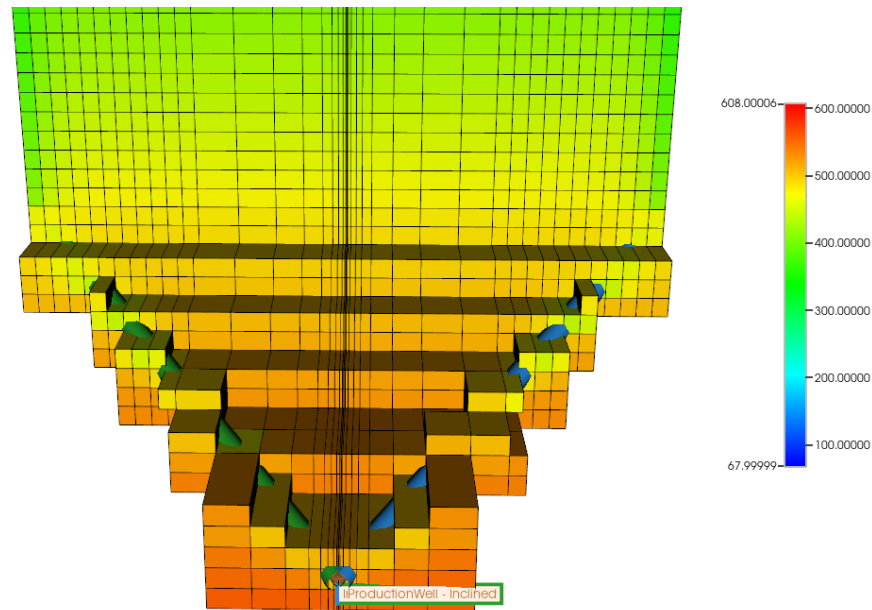


**Figure 20.** Reservoir temperature distribution after 20 years of operation for the inclined V-shaped closed-loop well configuration.

After 20 years, the model estimated a produced fluid temperature of 176 °F from an injected fluid temperature of 140 °F, as depicted in Figure 21, which shows the temperature profiles of the injection and production wells with depth. The temperature profiles show a slight decrease at shallower depths. For the injector well, the fluid temperature increases with depth, and for the production well, the fluid temperature decreases as the fluid flows upward. However, the inclined wellbore leads to an unsteady temperature increase, indicating less stability compared to the other models.

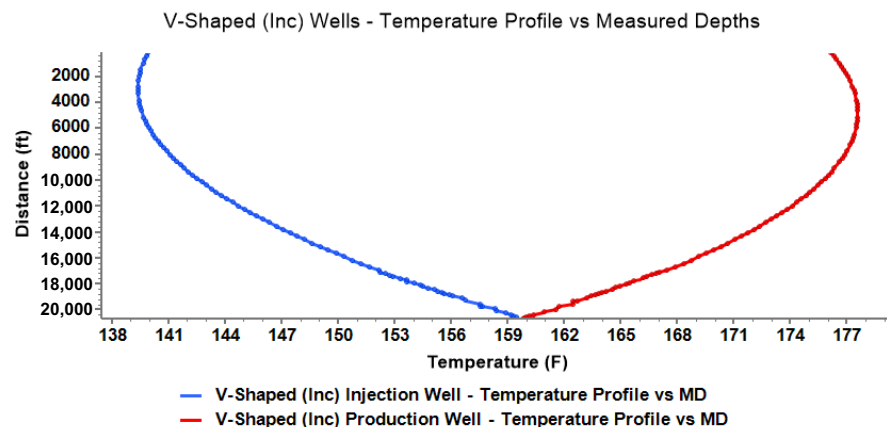


**Figure 21.** Estimated temperature profiles as a function of the measured depth for the injection and production wells, including the inclined V-shaped lateral well portion. The notation “V-Shaped (Inc) Wells” was used in the simulation case labeling and is retained in this plot.



### 3.6. Long-Term Performance Analysis of EGS Well Model

The EGS simulation model demonstrates outstanding performance in heat extraction compared with the previously presented well configurations. The hydraulic fractures extending from the injection well to the production well enhance the contact area between the injected fluid and the targeted formation depth, maximizing the heat transfer process (Figure 22). Here, we assume that all fractures contribute equally to fluid flow from the injection to the production wells.

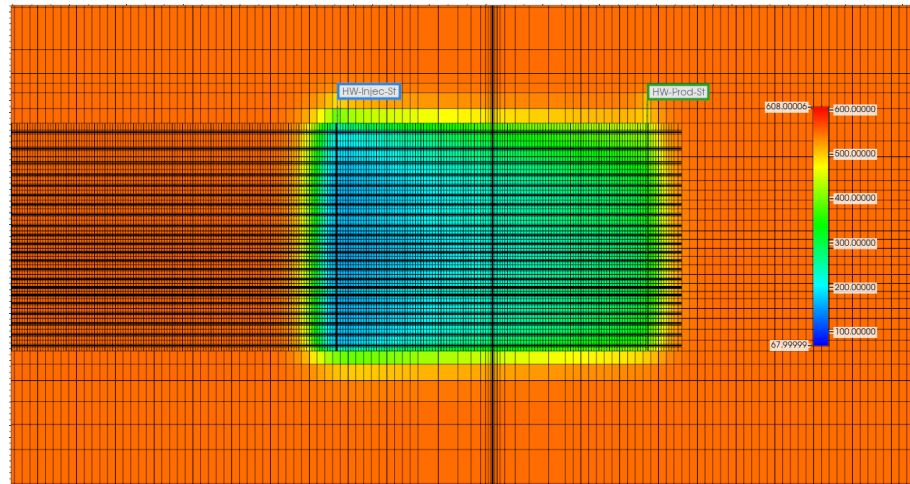


**Figure 22.** Reservoir temperature distribution after 20 years of operation for the EGS well configuration.

After 20 years of operation, the EGS model estimated a produced fluid temperature of 446 °F, marking a substantial increase from the injected fluid temperature of 140 °C. Water remains in the liquid phase under all operational conditions. Figure 23 presents the temperature profiles for the injection and production wells, showing a significant difference between the bottom hole temperatures for each well. The distance between the wells and the greater surface area provided by the hydraulic fractures allows for more efficient heat transfer from the HRD to the flowing fluid, resulting in a significant fluid temperature increase between the injection and production wells. The fluid temperature at the exit of the injection well is 160 °F, while the fluid temperature entering the production well is 540 °F, which is closer to the original reservoir temperature of 574 °F. The high produced temperature achieved underscores the potential of EGS technologies to effectively access and utilize deeper and hotter geothermal resources.

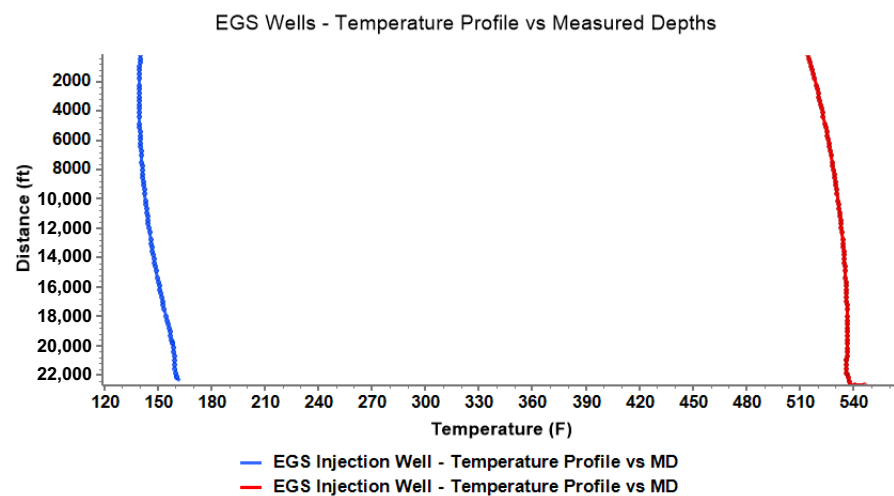


**Figure 23.** Estimated temperature profiles as a function of the measured depth for the injection and production wells in the EGS model.

### 3.7. Long-Term Performance Analysis of Inclined EGS Well Model

The inclined EGS well model shows similar behavior to the EGS model in terms of the reservoir temperature distribution between the injection and production wells. The cold fluid injected flows through the hydrate fractures, extracting heat from the HDR and increasing its temperature. Over time, the reservoir temperature decreases because of heat transfer from the HDR to the flowing fluid (Figure 24).

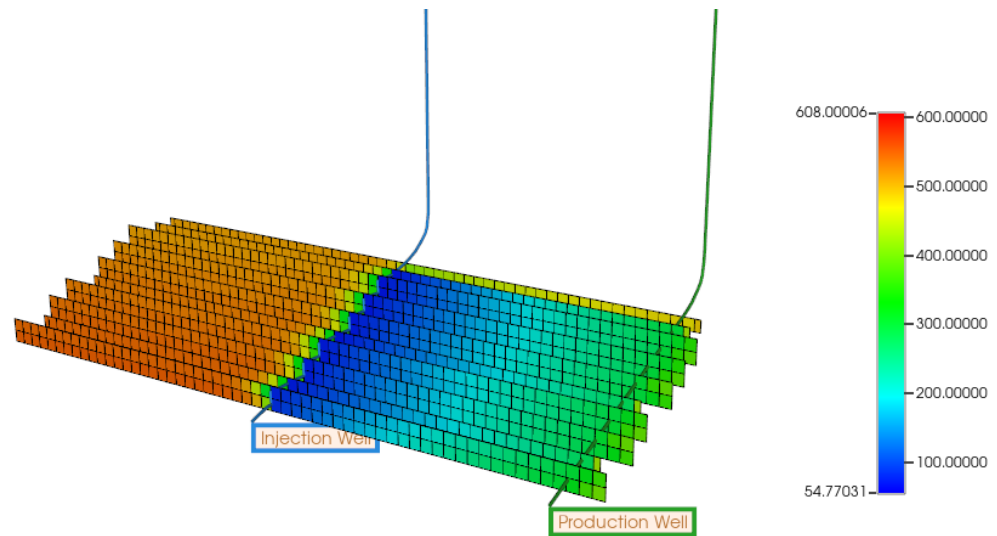


**Figure 24.** Reservoir temperature distribution after 20 years of operation predicted by the inclined EGS model.

After 20 years of operation, the model estimated a produced fluid temperature of 425 °F. In this case, the increase in the produced fluid temperature is lower than that obtained by the EGS model. In the inclined EGS model, the inclined lateral section starts at a shallower depth and ends at the target depth at the toe of the lateral section. The initial temperature in the lateral section follows the geothermal gradient, with a lower temperature at the heel and a higher temperature at the toe. This well configuration leads to the production of less thermal energy compared to the EGS model with horizontal lateral sections at the target depth, as indicated by a lower produced fluid temperature. Figure 25 presents the estimated temperature profiles as a function of the measured depth for the injection and production wells after 20 years of operation. The temperature of the injected fluid increases with depth. Since the toe of the injection well is beyond the hydraulic fractures, this point of the reservoir maintains a higher temperature close to the initial reservoir temperature of 574 °F. At the production well, the produced fluid loses temperature as it flows up the well. Although it performs slightly below the standard EGS model, the inclined EGS model design enhances reservoir permeability through hydraulic fractures and facilitates extensive heat extraction, maintaining stable temperature and pressure profiles, and proving reliable for geothermal energy extraction.

The inclined EGS design would overcome drilling challenges by having a moderate turn from the original vertical trajectory, demonstrating the potential of inclined configurations to efficiently exploit geothermal energy under challenging conditions. This design choice, while slightly reducing efficiency, showcases the model's adaptability and effectiveness in geothermal extraction.

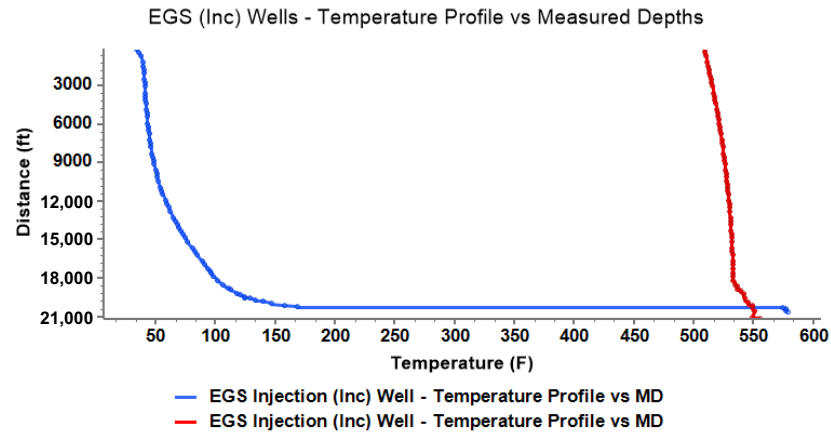


**Figure 25.** Estimated temperature profiles as a function of the measured depth for the injection and production wells in the inclined EGS model. The notation “EGS (Inc) Wells” was used in the simulation case labeling and is retained in this plot.

**Model Discussion**

The analysis of closed-loop and EGS models reveals significant differences in efficiency and performance across geothermal well configurations. The closed-loop systems, including U-shaped, V-shaped, inclined V-shaped, and PIP models, operate within a relatively narrow temperature range, with the V-shaped model showing a slight thermal advantage due to the longer residence time of injected fluid at the deepest part of the well (Figure 26). This illustrates the impact of design complexity on thermal extraction efficiency, balancing simplicity against performance enhancements.

In contrast, the EGS and inclined EGS models exhibit substantially higher produced fluid temperatures (Figure 27), benefiting from the increased surface area for heat conduction provided by the hydraulic fractures. Despite the slight decrease in thermal efficiency due to the inclined design, both EGS configurations significantly outperform the closed-loop models, demonstrating the effectiveness of EGS technology in accessing deeper geothermal resources. However, there is a continuous decrease in output temperature in the EGS configurations due to the cooling of the reservoir rock over time.

A comprehensive overview, presented in Figure 28, compares all models, clearly highlighting the superior performance of EGS systems over traditional closed-loop configurations. While the U-shaped and V-shaped models achieve moderate temperature gains, specialized modifications like fracturing in the U-shaped (fracked high-conductivity) models significantly boost performance.

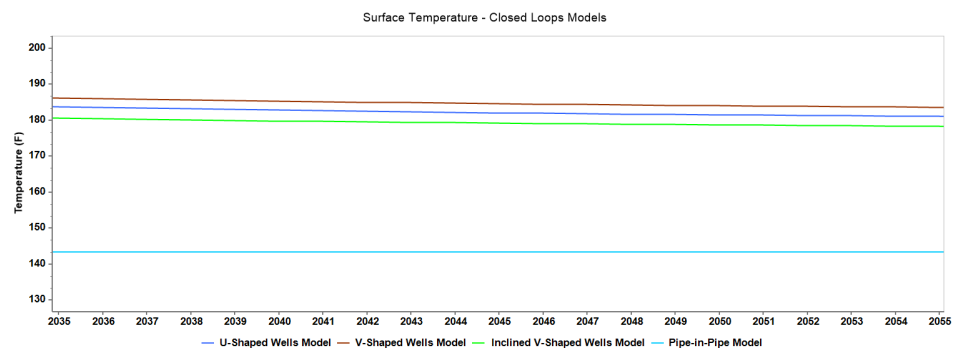


**Figure 26.** Comparison of produced surface temperatures of closed-loop well configurations after 20 years.

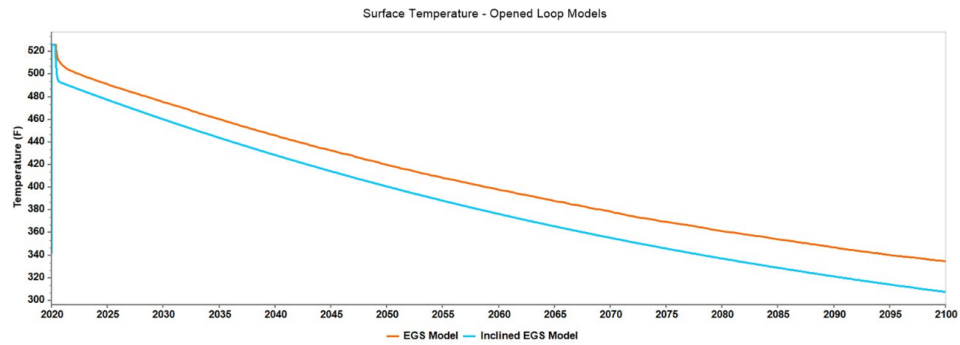


Figure 27. Estimated produced surface temperatures by EGS and inclined EGS models after 20 years.

## Simulation Results

Comparison [All Geothermal Wells Models]

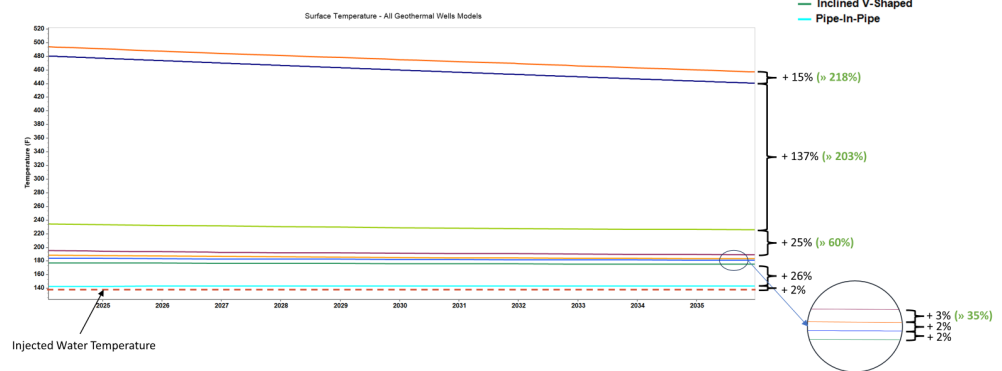


Figure 28. Comparison of overall produced surface temperatures of all geothermal well configurations after 20 years.

The temperature increases ( $\Delta T$ ) across the models vary, with the PIP model showing a minimal +3 °F increase, underscoring its limited efficiency. Meanwhile, the EGS models display dramatic increases of +306 °F and +285 °F, exemplifying their potent high-temperature extraction capabilities (Table 5). This stark contrast underscores the effectiveness of EGS systems in harnessing high-temperature geothermal energy, further enhanced by fracturing and material innovations in certain models. This analysis not only highlights the performance variability among geothermal configurations but also emphasizes the potential for significant enhancements in traditional systems through innovative techniques. Moreover, it reaffirms the high thermal efficiencies achievable with EGS systems, positioning them as ideal for deep geothermal energy extraction. These findings are vital for guiding future research and development in optimizing geothermal extraction techniques to maximize energy capture and efficiency in the renewable energy sector.

Table 5. Comparison of well models’ temperature performance.

Well Model	Surface Temperature (°F)	$\Delta T$ (°F)
Pipe-in-Pipe	143	+3
Inclined V-Shaped	179	+39
U-Shaped	182	+42
V-Shaped	185	+45
U-Shaped (Fracked Closed)	189	+49
U-Shaped (Fracked Opened)	225	+85
Inclined EGS	425	+285
EGS	446	+306

#### 4. Summary and Conclusions

This study provided an exhaustive numerical modeling analysis of diverse geothermal well configurations in the Wattenberg formation, using the CMG-STARS thermal reservoir simulation software to evaluate their thermal efficiency and potential for electricity generation.

This study encompassed traditional closed-loop geothermal (CLG) systems like pipe-in-pipe and U-shaped designs, alongside innovative setups such as hybrid models that combine closed-loop and open-loop features through hydraulic fracturing and high-conductivity material injections.

This study highlighted moderate thermal performance across traditional CLG systems but showed significant enhancements in U-shaped models through the hybrid system, markedly improving their delta temperature ( $\Delta T$ ) values.

The enhanced geothermal system (EGS) configurations, including standard and inclined EGSs, demonstrated exceptional heat extraction capacities suitable for electricity generation in the deeper and more complex reservoirs of the DJ Basin, with  $\Delta T$  values of +306 °F and +285 °F, respectively.

These findings suggest that while EGS models offer superior performance, their implementation requires careful consideration of geological and technical challenges to ensure sustainable energy output.

**Author Contributions:** Conceptualization, L.E.Z.; methodology, A.N. and L.E.Z.; validation, A.N. and L.E.Z.; formal analysis, A.N. and L.E.Z.; investigation, A.N. and L.E.Z.; resources, L.E.Z.; writing—original draft preparation, A.N.; writing—review and editing, L.E.Z.; supervision, L.E.Z.; project administration, L.E.Z.; funding acquisition, L.E.Z. All authors have read and agreed to the published version of the manuscript.

**Funding:** This research was funded by the Rock and Fluid Multiphysics Consortium of the Colorado School of Mines.

**Data Availability Statement:** The data that support the findings of this study are available on request from the corresponding author. The data are not publicly available due to privacy or ethical restrictions.

**Conflicts of Interest:** The authors declare no conflicts of interest.

#### Abbreviations

The following abbreviations are used in this manuscript:

CLGS	Closed-loop geothermal system
CMG	Computer Modeling Group
DJ	Denver-Julesburg
EGSs	Enhanced geothermal systems
HDR	Hot Dry Rock
PIP	Pipe-in-pipe
UBA	User Block Address

#### References

- Cheng, Y.; Zhang, Y.; Yu, Z.; Hu, Z.; Ma, Y.; Yang, Y. Experimental and numerical studies on hydraulic fracturing characteristics with different injection flow rates in granite geothermal reservoir. *Energy Sci. Eng.* **2021**, *9*, 142–168. [[CrossRef](#)]
- Pratama, H.B.; Saptadji, N.M. Study of Production-Injection Strategies for Sustainable Production in Geothermal Reservoir Two-Phase by Numerical Simulation. *Indones. J. Geosci.* **2021**, *8*, 25–38.
- Simmons, S.F.; Allis, R.G.; Kirby, S.M.; Moore, J.N.; Fischer, T.P. Interpretation of hydrothermal conditions, production-injection induced effects, and evidence for enhanced geothermal system-type heat exchange in response to 30 years of production at Roosevelt Hot Springs, Utah, USA. *Geosphere* **2021**, *17*, 1997–2026. [[CrossRef](#)]
- Xu, T.; Zhao, Y.; Zhao, J.; Zhang, L.; Liu, S.; Liu, Z.; Feng, B.; Feng, G.; Yue, G. Heat Extraction Performance and Optimization for a Doublet-well Geothermal System in Dezhou, China. *Energy Explor. Exploit.* **2022**, *40*, 619–638. [[CrossRef](#)]
- Chen, G.; Jiao, J.J.; Jiang, C.; Luo, X. Surrogate-assisted level-based learning evolutionary search for geothermal heat extraction optimization. *Renew. Sustain. Energy Rev.* **2024**, *189*, 113860. [[CrossRef](#)]
- Majer, E.L.; Baria, R.; Stark, M.; Oates, S.; Bommer, J.; Smith, B.; Asanuma, H. Induced seismicity associated with Enhanced Geothermal Systems. *Geothermics* **2007**, *36*, 185–222. [[CrossRef](#)]

7. Abdelrahman, K.; Ekwok, S.E.; Ulem, C.A.; Eldosouky, A.M.; Al-Otaibi, N.; Hazaea, B.Y.; Hazaea, S.A.; András, P.; Akpan, A.E. Exploratory mapping of the geothermal anomalies in the neoproterozoic Arabian Shield, Saudi Arabia, using magnetic data. *Minerals* **2023**, *13*, 694. [[CrossRef](#)]
8. Zhang, C.; Feng, Q.; Zhang, L.; Qin, S.; Jiang, G.; Hu, J.; Hu, S.; Huang, R.; Zhang, H. Characteristics of Radiogenic Heat Production of Widely Distributed Granitoids in Western Sichuan, Southeast Tibetan Plateau. *Lithosphere* **2022**, *2022*, 4165618. [[CrossRef](#)]
9. Robson, S.G.; Banta, E.R. *Geology and Hydrology of the Deep Bedrock Aquifers in Eastern Colorado*; Report 85-4240; US Geological Survey: Reston, VA, USA, 1987.
10. Schulz, S.U. *Investigations on the Improvement of the Energy Output of a Closed Loop Geothermal System (CLGS)*; Technische University: Berlin, Germany, 2008.
11. Cui, G.; Ren, S.; Zhang, L.; Ezekiel, J.; Enechukwu, C.; Wang, Y.; Zhang, R. Geothermal exploitation from hot dry rocks via recycling heat transmission fluid in a horizontal well. *Energy* **2017**, *128*, 366–377. [[CrossRef](#)]
12. Song, X.; Shi, Y.; Li, G.; Yang, R.; Wang, G.; Zheng, R.; Li, J.; Lyu, Z. Numerical simulation of heat extraction performance in enhanced geothermal system with multilateral wells. *Appl. Energy* **2018**, *218*, 325–337. [[CrossRef](#)]
13. Jiang, H.; Guo, L.; Kang, F.; Wang, F.; Cao, Y.; Sun, Z.; Shi, M. Geothermal Characteristics and Productivity Potential of a Super-Thick Shallow Granite-Type Enhanced Geothermal System: A Case Study in Wendeng Geothermal Field, China. *Sustainability* **2023**, *15*, 3551. [[CrossRef](#)]
14. Kazemi, A.; Mahbaz, S.; Dehghani-Sanij, A.; Dusseault, M.; Fraser, R. Performance Evaluation of an Enhanced Geothermal System in the Western Canada Sedimentary Basin. *Renew. Sustain. Energy Rev.* **2019**, *113*, 109278. [[CrossRef](#)]
15. Song, X.; Shi, Y.; Li, G.; Shen, Z.; Hu, X.; Lyu, Z.; Zheng, R.; Wang, G. Numerical analysis of the heat production performance of a closed loop geothermal system. *Renew. Energy* **2018**, *120*, 365–378. [[CrossRef](#)]
16. Bu, X.; Jiang, K.; Li, H. Performance of geothermal single well for intermittent heating. *Energy* **2019**, *186*, 115858. [[CrossRef](#)]
17. Zhang, Y.; Yu, C.; Li, G.; Guo, X.; Wang, G.; Shi, Y.; Peng, C.; Tan, Y. Performance analysis of a downhole coaxial heat exchanger geothermal system with various working fluids. *Appl. Therm. Eng.* **2019**, *163*, 114317. [[CrossRef](#)]
18. Wang, G.; Song, X.; Shi, Y.; Zheng, R.; Li, J.; Li, Z. Production performance of a novel open loop geothermal system in a horizontal well. *Energy Convers. Manag.* **2020**, *206*, 112478. [[CrossRef](#)]
19. Frash, L.P.; Meng, M.; Bijay, K. Greenfield Reservoir Engineering for the Wattenberg Field with Comparison of Advanced, Enhanced, and Caged Geothermal Systems. In Proceedings of the 49th Workshop on Geothermal Reservoir Engineering Stanford University, Stanford, CA, USA, 12–14 February 2024.
20. Won, J.; Choi, H.J.; Lee, H.; Choi, H. Numerical investigation on the effect of cementing properties on the thermal and mechanical stability of geothermal wells. *Energies* **2016**, *9*, 1016. [[CrossRef](#)]
21. Norbeck, J.; Latimer, T. Commercial-Scale Demonstration of a First-of-a-Kind Enhanced Geothermal System. *arXiv* **2023**. [[CrossRef](#)]

**Disclaimer/Publisher’s Note:** The statements, opinions and data contained in all publications are solely those of the individual author(s) and contributor(s) and not of MDPI and/or the editor(s). MDPI and/or the editor(s) disclaim responsibility for any injury to people or property resulting from any ideas, methods, instructions or products referred to in the content.